



ELSEVIER

Available online at [www.sciencedirect.com](http://www.sciencedirect.com)

SCIENCE @ DIRECT®

Nuclear Instruments and Methods in Physics Research A ■■■■■ ■■■■■

**NUCLEAR  
INSTRUMENTS  
& METHODS  
IN PHYSICS  
RESEARCH**  
Section A[www.elsevier.com/locate/nima](http://www.elsevier.com/locate/nima)

# An innovative concept for acceleration of low-energy low-charge-state heavy-ion beams<sup>☆</sup>

P.N. Ostroumov, A.A. Kolomiets, S. Sharma, N.E. Vinogradov\*, G.P. Zinkann

*Argonne National Laboratory, Physics Division, 9700 S. Cass Ave., Bldg. 203, H-149, Argonne IL 60439, USA*

Received 17 January 2005; received in revised form 14 March 2005; accepted 19 March 2005

## Abstract

A new accelerating structure called Hybrid RFQ (H-RFQ) is suggested. The structure consists of an alternating series of drift tubes (DTLs) and radio frequency quadrupole (RFQ) sections incorporated into one resonator. The proposed approach allows one to achieve twice as much average accelerating gradient compared to a conventional RFQ. A particular version of a 12.125 MHz H-RFQ has been developed for the Rare Isotope Accelerator (RIA) (Nolen, Nucl. Phys. A 734 (2004) 661–668; Ostroumov et al., Nucl Instr. and Meth. B 204 (2003) 433–439). A half-scale model of this structure has been built and studied to determine the final specifications for the full-power prototype. This paper presents comprehensive beam dynamics studies in a H-RFQ accelerating structure and experimental investigations of the 12.125 MHz H-RFQ model. Possible applications of H-RFQ structures are discussed.

© 2005 Published by Elsevier B.V.

PACS: 29.17.+w; 29.27.–a; 07.05.Tp

Keywords: Heavy-ion beam; Radio frequency quadrupole; Drift tube; Beam dynamics; Cold model

## 1. The Hybrid radio frequency quadrupole (RFQ) concept

Drift tube (DTL) structures have been widely utilized for acceleration of ion beams. However, it is difficult to achieve a required transverse focus-

ing strength in the case of low-charge-state, heavy-ion beams due to the low charge-to-mass ratio  $q/A$ . Use of magnetic focusing elements in a limited space inside the DTLs is not effective for low- $q$ , heavy-ion beams. A conventional RFQ accelerator is more suitable in this case. The RF electric fields of such devices are very effective at focusing heavy ions, but the longitudinal electric field provided only by the vane modulation makes it an inefficient accelerating structure. For low-velocity ions, the RFQ must operate at a very low RF

<sup>☆</sup>This work is supported by the U.S. Department of Energy under contract W-31-109-ENG-38.

\*Corresponding author. Tel.: +1 630 252 5643.

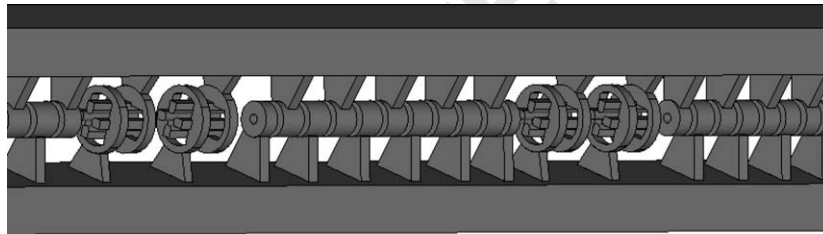
E-mail address: [vinogradov@phy.anl.gov](mailto:vinogradov@phy.anl.gov) (N.E. Vinogradov).

1 frequency leading to a very large and expensive  
 2 machine. A possible way to enlarge the accelerat-  
 3 ing gradient was originally proposed in a spatially  
 4 periodic RFQ, which consists of DTLs with  
 5 “horns” forming quadrupole-focusing fields in  
 6 the gaps [1]. An analogous approach is implemen-  
 7 ted in RF-focused drift-tube (RFD) structures [2]  
 8 by configuring the DTLs as two independent  
 9 pieces thus producing the RF quadrupole fields  
 10 inside the tubes. It is especially attractive because  
 11 DTL structure usually provides much higher  
 12 accelerating efficiency compared to the conven-  
 13 tional RFQ due to the improved accelerating field  
 14 distribution and maximized transit time factor.  
 15 The alternative way to utilize this advantage of a  
 16 DTL structure is use of a hybrid structure with  
 17 accelerating and focusing zones separated in space.  
 18 The idea of separate accelerating and focusing  
 19 zones was first implemented in IH-DTL structures  
 20 [3] that have been developed and used for ion  
 21 beams with  $q/A \geq \frac{1}{60}$  in an energy range above

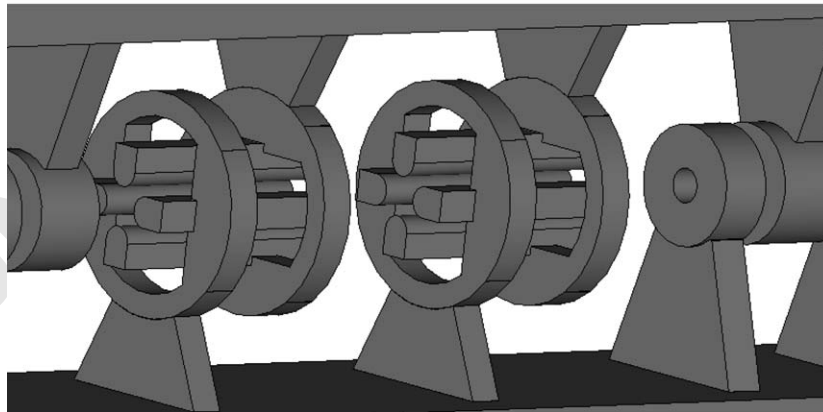
49 120 keV/u. The IH-DTL structures consist of a  
 50 series of DTL accelerating sections each followed  
 51 by an independent DC magnetic focusing triplet.  
 52 The triplets can be located either inside or outside  
 53 of the resonator tank.

54 We have found that a similar concept can be  
 55 successfully applied for very-low-energy ion beams  
 56 with  $q/A \geq \frac{1}{238}$  if the RFQ elements are used for  
 57 transverse focusing. Incorporating the DTL accel-  
 58 erating and RFQ focusing sections into one  
 59 resonator allows us to form a compact hybrid  
 60 structure that we call the Hybrid RFQ (H-RFQ)  
 61 [4], see Fig. 1.

62 The focusing section of the H-RFQ is formed by  
 63 RFQ cells with length  $\beta\lambda/2$  and can include one or  
 64 several cells. The required focusing strength is  
 65 provided by an appropriate value of an average  
 66 radius  $R_{0i}$  in each cell for the given inter-electrode  
 67 voltage. The focusing effect of the RFQ cell is  
 68 equivalent to a magnetic quadrupole with an  
 69 effective length  $\beta\lambda/2$  if



(a)



(b)

Fig. 1. Hybrid RFQ structure formed by alternating series of RFQ and drift tube sections (a) and a possible configuration of the RFQ focusing section (b).

$$R_{0i} = \sqrt{\frac{2U_1}{\pi\beta c G_m}}, \quad (1)$$

where  $U_1$  is the electric potential on the RFQ electrodes and  $G_m$  is the equivalent magnetic gradient. The left column in Fig. 2 represents an example of the focusing zone design. It consists of two RFQ sections each with length  $\beta\lambda$  separated by a drift space  $\beta\lambda/2$ . The focusing strength of each RFQ lens with the length  $\beta\lambda/2$  is defined by the aperture radius  $R_{0i}$ . Each two-cell RFQ section acts as a “doublet”. The drift space between the “doublets” changes the sign of the focusing fields; therefore, the entire focusing zone works as a symmetric triplet. Similar properties of the transverse beam dynamics can be obtained without drift space (FDFD combination, middle column in Fig. 2) or in “triplet” focusing zone consisting of three  $\beta\lambda/2$  RFQ cells (FDF combination, right column in Fig. 2). The latter requires higher values of effective magnetic gradient  $G_m$ . To eliminate the fringing field effects in the RFQ section, a gap between the DTL and RFQ zones must be chosen to match the arrival time of the bunches to a zero field at the edges of the RFQ electrodes.

The H-RFQ concept assumes that the focusing elements are not employed within the DTL

sections. In the case of very-low-energy beams, the first DTL zone should be short to avoid strong defocusing effect of the accelerating field. Using alternating phase focusing (APF) is an acceptable approach to evade this negative aspect. In APF, the defocusing effect is compensated by a combination of gaps with an opposite sign of the synchronous phase [5]. However, the average absolute value of synchronous phase can be quite large, which reduces the total energy gain in such a DTL zone. Another possible technique is the use of zero equilibrium synchronous phase for well-bunched beams [6]. In most cases, DTL sections can be designed for given negative synchronous phase.

## 2. H-RFQ for the Rare Isotope Accelerator (RIA) Post-Accelerator

A modern post-accelerator for rare isotopes must produce high-quality beams of radioactive ions over full mass range up to mass 238. To provide the highest possible intensity of beams available for experiments, the injector section of the Post-Accelerator for the RIA facility [7] requires acceleration of singly charged ions at

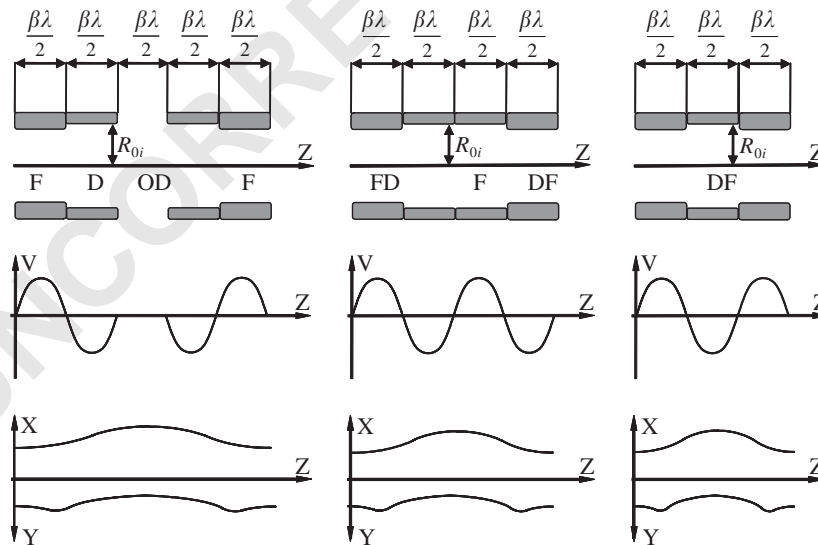


Fig. 2. RFQ cells configuration, voltage distribution and beam envelopes for the case of FDODF combination (left column), FDFD combination (middle column) and FDF combination (right column).

Table 1

Basic design parameters of the H-RFQ

Operating frequency	12.125 MHz
Singly charged mass range	6–238
Beam energy	7.12–20.61 keV/u
Length	334 cm
Number of drift tubes in DTL sections	13–10–13
Drift tube aperture radius	1.0 cm
RFQ aperture radius	1.09–1.23 cm
Inter-electrode voltage	100 kV
RF power according to the MWS	11.6 kW
Peak surface field	109 kV/cm

initial injection [8]. The efficient capture of a DC beam, while maintaining low longitudinal emittance, and initial acceleration up to 7 keV/u will be performed by using a multi-harmonic buncher and a conventional RFQ operating at 12.125 MHz [9]. The main requirement to the subsequent accelerating structure is the maximum energy gain at an acceptable maximum field strength, and low cost. To achieve these goals, a cw normally conducting linac for acceleration of singly charged uranium in the injector section of the RIA Post-Accelerator has been designed utilizing the H-RFQ concept. The whole H-RFQ structure consists of three DTL sections, where the beam is accelerated, and two RFQ sections with unmodulated electrodes where the beam is focused without acceleration. Each RFQ zone is formed by four RFQ cells with a  $\beta\lambda/2$ -gap in the middle (FDODF combination). In the first DTL section, the acceleration is provided with zero equilibrium synchronous phase while the second and third DTL zones operate at  $-20^\circ$  synchronous phase. The choice of 100 kV inter-electrode voltage is based on the operational experience with the 12.125 MHz RFQ [10]. Basic design parameters of the H-RFQ are given in Table 1. The main advantages of the proposed structure are as follows:

- higher accelerating gradient compared to a conventional RFQ structure;
- insensitivity of the focusing strength to the ion velocity;
- simplicity and cost-efficiency of the focusing elements;

- single power source for both accelerating and focusing elements;
- moderate length of the whole structure.

### 2.1. Beam dynamics design of the H-RFQ

Two independent tracking codes were applied for beam dynamics design of the H-RFQ. Preliminary simulations were performed by DYNAMION [11]. This code provides calculations of 2D electrical fields in the gaps between DTLs and transverse electric fields between RFQ electrodes. The code SIMION 7 [12] has been used to simulate 3D electric fields between the RFQ electrodes and neighboring DTLs. The choice of  $R_{0i}$  for each RFQ cell was carried out using the TRACE code characterizing the RFQ cells by equivalent magnet quadrupoles. For the complete test of beam dynamics, we have applied the tracing code TRACK [13] with a realistic representation of 3D electric fields. The code SUPERFISH was used to calculate axi-symmetric electrical field in the DTL zones, while accurate simulations of 3D field in the RFQ sections were obtained by the CST EM Studio code [14]. Such an approach has allowed us to use 3D fields for the beam dynamics design. These precise simulations have revealed that some corrections of the RFQ electrodes geometry with respect to the initial design were necessary to provide the required properties of the beam dynamics. Beam envelopes and phase space plots after the final adjustment of the structure geometry are shown in Fig. 3.

Fig. 4 shows beam energy as a function of the distance in the H-RFQ and in the conventional RFQ. The reference RFQ was designed at the same voltage and operating frequency with constant phase advance of transverse oscillations per period equal to  $17^\circ$ . As is seen from the graph, the H-RFQ provides almost twice as much accelerating voltage. The peak surface electric field occurs on the first RFQ cell and is 20% lower than in the existing 12 MHz RFQ [9]. The surface field on the DTLs is kept even lower by selecting long accelerating gaps. Numerical simulations have not detected any transverse emittance growth.

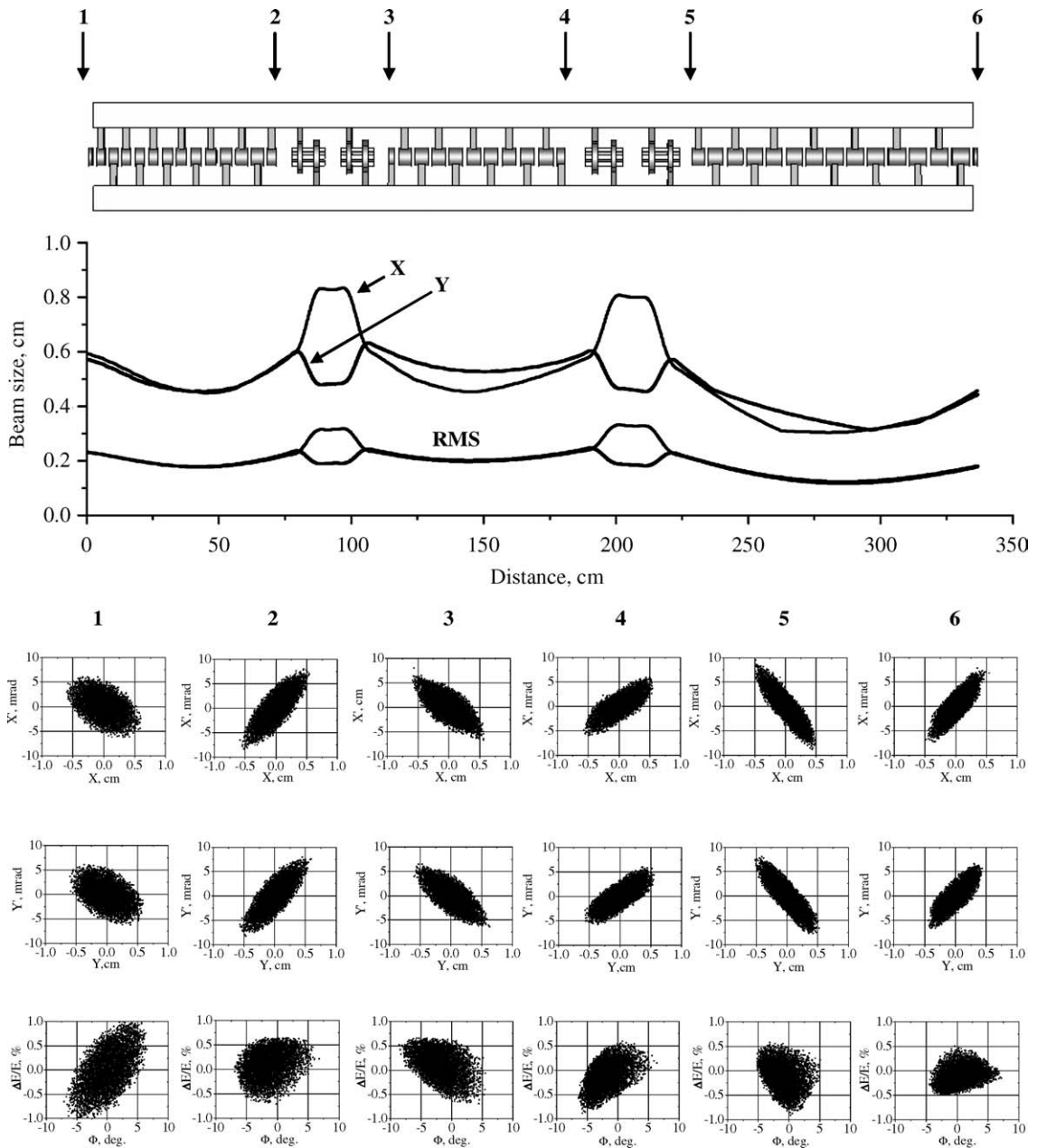


Fig. 3. Beam envelopes and phase space plots simulated for 5000 particles; input total transverse emittance is  $0.15\pi$  mm mrad, input longitudinal emittance is  $0.1\pi$  keV/u ns.

The 100% transmission transverse acceptance of the H-RFQ is  $0.2\pi$  mm mrad, which is twice the maximum beam emittance expected for light exotic ions in the RIA Post-Accelerator. Fig. 5 shows

longitudinal emittance growth for 99.5% of particles as a function of the input transverse emittance. The emittances of the most radioactive beams are expected to be very low due to the high-

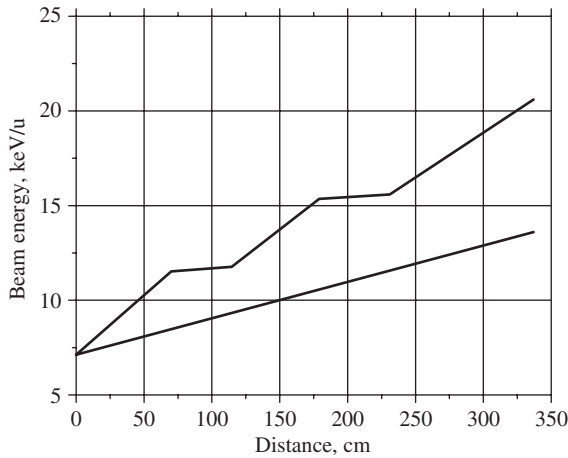


Fig. 4. Energy gain in the H-RFQ compared to a conventional RFQ.

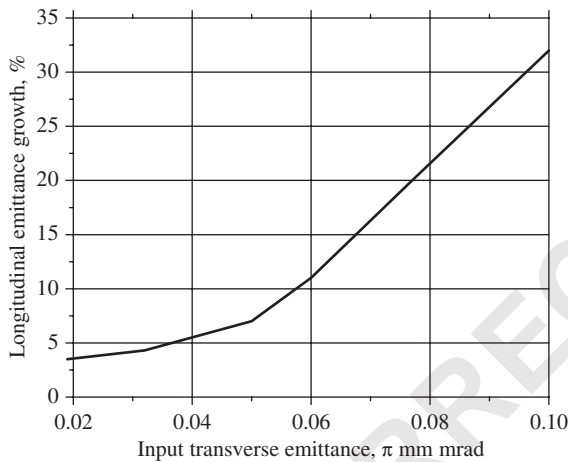


Fig. 5. Longitudinal emittance growth in the H-RFQ as a function of input transverse emittance.

resolution isobar separator [15]; therefore, the growth of 99.5% in longitudinal emittance will be below 7%. In the H-RFQ, beam parameters such as average energy, emittances, Twiss parameters, etc. experience negligible change if the voltage error is in the range  $\pm 3\%$  from the nominal value.

## 2.2. Electrodynamics design of the H-RFQ

In order to provide the required properties of the H-RFQ structure, a new design of a

12.125 MHz resonator was proposed. The structure consists of four quarter-wave resonators strongly coupled through the capacitance between DTLs (see Fig. 6). It also can be interpreted as a symmetric Wideroe structure [16]. This type of resonator allows us to provide the required 12.125 MHz resonant frequency with a compact cavity. The wavelength is larger than the typical resonator dimension by the factor 10; therefore, uniform voltage distribution along the structure was expected. In addition, the structure is mechanically stable for such a low frequency.

The simulations of the H-RFQ resonant structure have been performed using CST MW Studio code [17]. It was found that for the copper cavity the RF losses are less than 12 kW at 100 kV inter-electrode voltage. In this structure, the losses are lower than in a split-coaxial RFQ of a similar length because the total capacitive loading of the DTLs is about half compared to the four-vane structure. The measured voltage distribution on all gaps along the structure is uniform as was predicted. The required configuration of the transverse electric field in the RFQ sections has been achieved. The main difficulty in these simulations was that the sizes of DTLs, gaps, and RFQ electrodes are small compared to overall dimensions of the cavity. This difference required a large number of mesh cells for the simulations which resulted in an unacceptable calculation time, and the frequency solution was non-convergent. To overcome this problem, some simplifications of the shape of the structure details had to be implemented. With these simplifications, a frequency error in the simulations was expected and the developed design necessitated an experimental test.

## 3. Half-scale aluminum cold model of the 12.125 MHz H-RFQ

### 3.1. Construction of the H-RFQ prototype

A half-scale (24.25 MHz) aluminum cold model of the H-RFQ (see Fig. 7) has been designed, built and tested [18] to determine the final resonator dimensions, accelerating and focusing field dis-

49  
51  
53  
55  
57  
59  
61  
63  
65  
67  
69  
71  
73  
75  
77  
79  
81  
83  
85  
87  
89  
91

93  
95

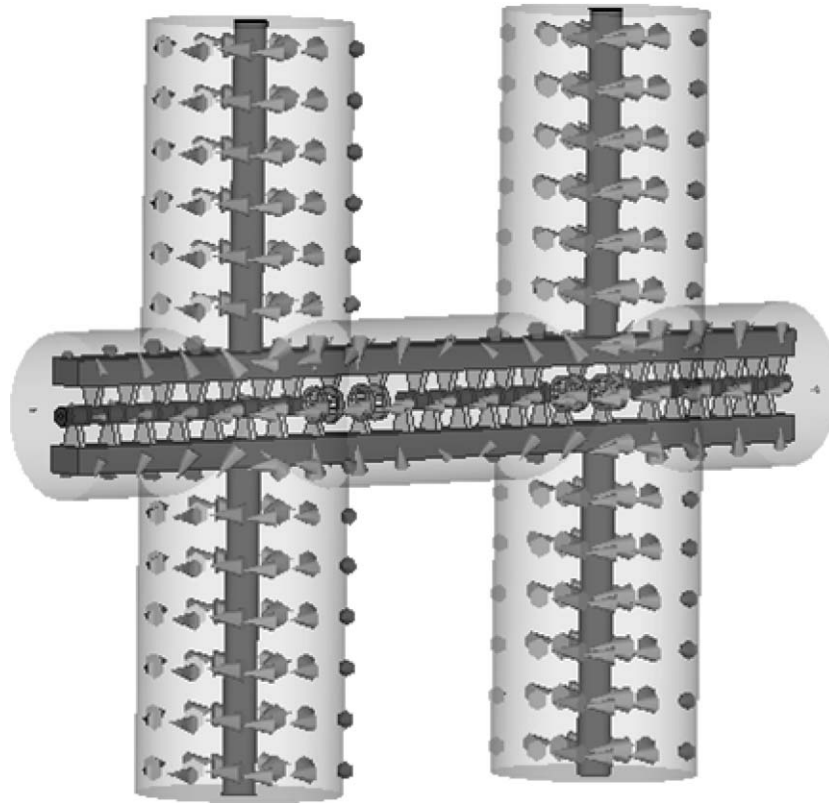


Fig. 6. Resonant structure of the 12.125 MHz H-RFQ in Micro Wave Studio model. Arrows show the magnetic field.

tribution, quality factor and coupling to the external power supply. The structure consists of two beams (upper and lower) with DTLs and RFQ electrodes connected to them as shown in Fig. 8. The tubes and RFQs situated on the same beam are aligned during fabrication and fixed by bolts. The beams are held by four vertical stems, which are connected to the covers of vertical coaxial stubs by holders incorporating alignment mechanisms. These mechanisms provide tuning of the gaps length and centering of the upper and lower sets of DTLs and RFQs with respect to the major axis of the structure. All flanges of the model are equipped with RF spring gaskets supplied by Bal Seal Engineering [19]. The end plate of each stub is moveable thus forming a frequency tuner. The same RF spring gaskets ensure good RF contacts between end plates, vertical stems and cavity walls. Two capacitive tuners are installed in the middle of

structure. Also, four additional tuners are mounted in the middle of each stub. The prototype is equipped with one pick-up loop installed in the upper stub and two driving loops: one in the upper and one in the lower stub.

### 3.2. Low-power tests

The first measurements of the electrodynamic parameters of the cavity revealed three important differences from the design:

- (1) the measured quality factor  $Q$  was 3.5 times lower than the calculated value, and was unstable;
- (2) the frequency was approximately 2 MHz above the design prediction;
- (3) a tilt in the field amplitude distribution in the third DTL section was measured.

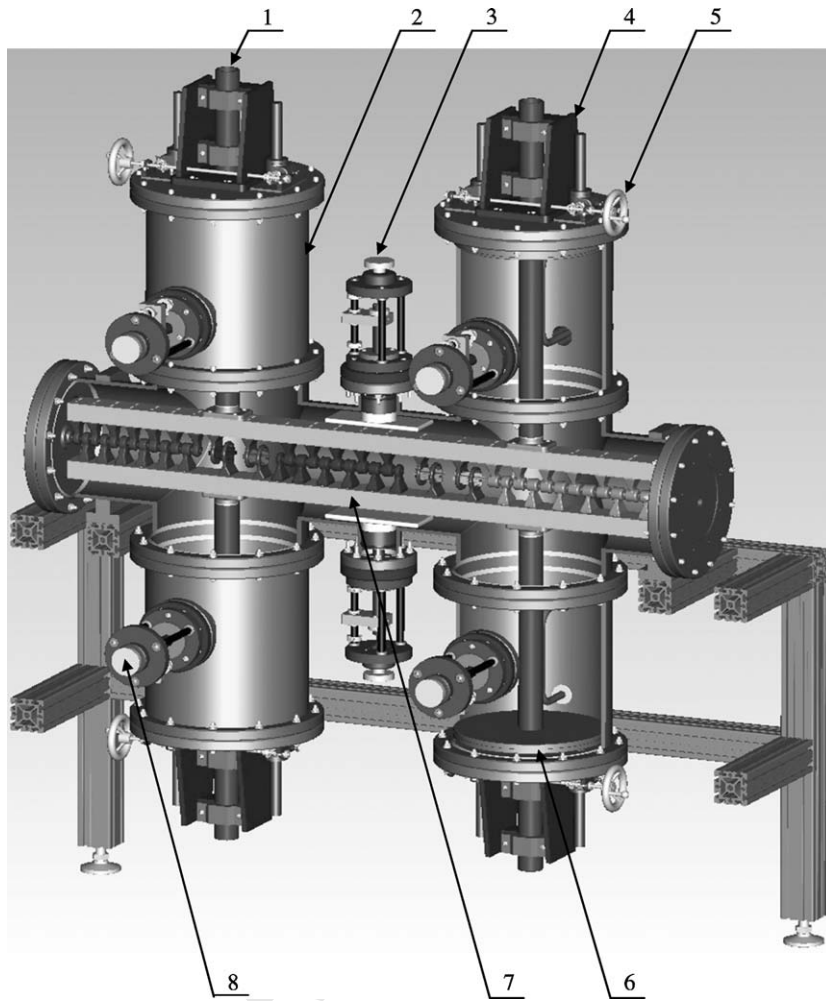


Fig. 7. 3D model of the H-RFQ prototype: 1—one of the four vertical stems, 2—one of the four stabs, 3—one of the two capacitive tuners, 4—one of the four stem holders with alignment mechanism, 5—one of the four end plate frequency tuners, 6—one of the four end plates, 7—one of the two horizontal beams with drift tubes and RFQs, 8—one of the four additional tuners.

The low and unstable quality factor was explained by poor RF contacts between moveable end plates, vertical stems and cavity walls. The contact between plate and stem is especially important for this resonator because the highest density of the surface current is achieved on the stem. The second and third circumstances were related to a low precision of the MWS Studio simulations in this particular problem as was mentioned above.

To address the low  $Q$ , the areas of RF contact were additionally treated, equipped with stiffer spring gaskets and covered by a special silver grease from Technit [20]. After the modifications, the quality factor became stable and achieved 70% of the calculated value for the material used for the resonator.

Next, we designed and built cylindrical inserts to the vertical stabs in order to tune the resonant frequency. The inserts were installed between the horizontal tank and the existing stabs using

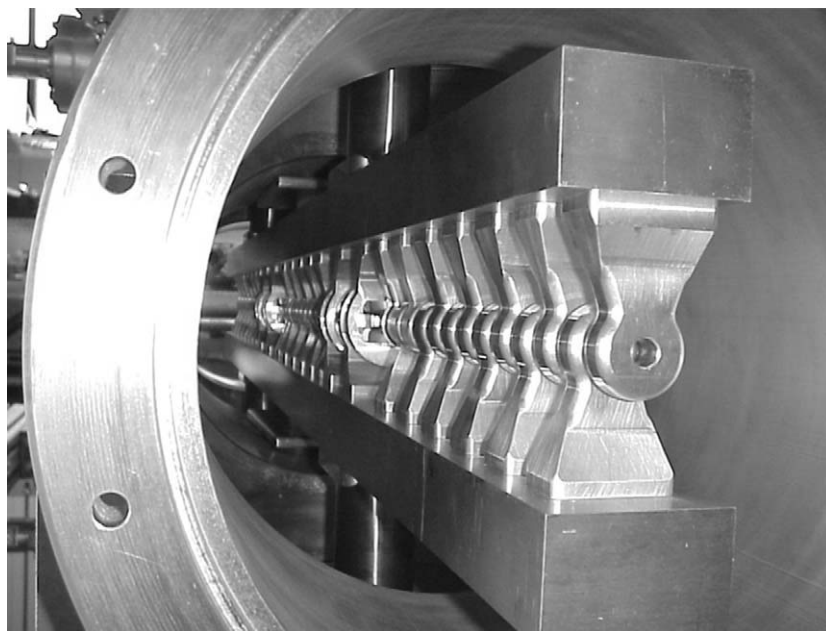


Fig. 8. Drift tubes and RFQ sections connected to beams.

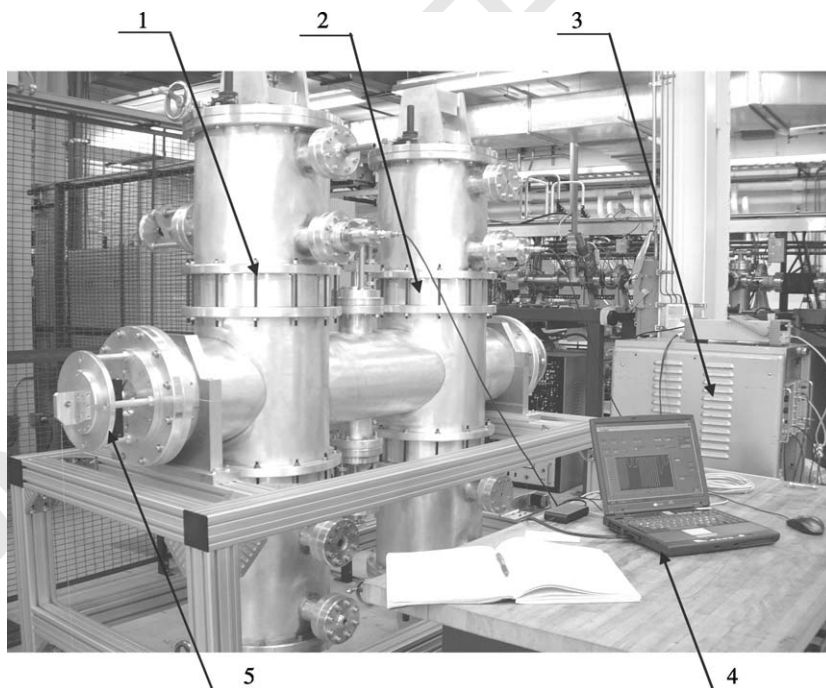


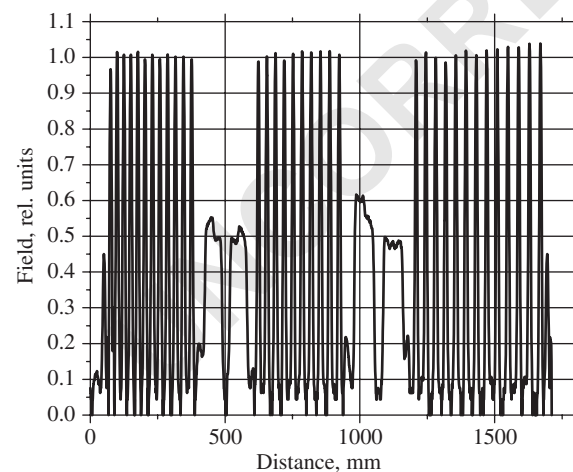
Fig. 9. H-RFQ cold model after the modifications: 1—tension rod; 2—one of the four cylindrical inserts, 3—equipment crate, 4—PC with bead-pull control system, 5—one of the two bead-pull alignment mechanisms.

1 tension rods. After these modifications were made,  
 2 the resonant frequency of the model was close to  
 3 the required frequency and fine tuning was  
 4 performed by the frequency tuners. A view of the  
 5 modified prototype with a bead-pull test bench is  
 6 shown in Fig. 9. The electrodynamic parameters of  
 7 the model are summarized in Table 2.

8 To solve the final problem with the tilt of the  
 9 field distribution, additional capacitive tuners were  
 10 designed and installed in an appropriate location.  
 11 With the addition of the capacitive tuners, the field  
 12 amplitude in the gaps became uniform along the  
 13 entire structure within  $\pm 2\%$  (see Fig. 10). The  
 14 latter is entirely acceptable from the beam  
 15 dynamics point of view.

17  
 18 Table 2  
 19 Electrodynamic parameters of the H-RFQ prototype

	MWS simulations	Experiment before the modification	Experiment after the modification
Resonant frequency (MHz)	24.6	26.5	24.25
Quality factor	4700	1300–2300	3150
$R_{sh}/Q$ (Ohm)	$7.1 \times 10^4$	—	$6.9 \times 10^4$



20  
 21  
 22  
 23  
 24  
 25  
 26  
 27  
 28  
 29  
 30  
 31  
 32  
 33  
 34  
 35  
 36  
 37  
 38  
 39  
 40  
 41  
 42  
 43  
 44  
 45  
 46  
 47 Fig. 10. Final distribution of the field amplitude in the gaps  
 along the whole H-RFQ structure measured by bead-pull  
 technique.

#### 4. Summary and conclusions

49  
 50  
 51 A H-RFQ accelerator for low-energy low-  
 52 charge-state heavy-ion beams has been proposed  
 53 and developed. The detailed studies of beam  
 54 dynamics in the H-RFQ structure have been  
 55 carried out. The studies confirmed the expected  
 56 advantages of the H-RFQ compared to a conven-  
 57 tional RFQ. The particular version of the  
 58 12.125 MHz H-RFQ accelerator along with the  
 59 electrodynamic design of the original resonator  
 60 has been developed as an injector part of the RIA  
 61 Post-Accelerator. The remarkable features of the  
 62 proposed structure are low RF power consump-  
 63 tion per unit length, possibility to operate in cw  
 64 regime in a wide range of applied RF power and  
 65 relatively high shunt impedance with moderate  
 66 dimensions of the cavity. A half-scale aluminum  
 67 cold model of 12.125 MHz H-RFQ has been built  
 68 and studied. The required corrections of the cavity  
 69 design have been implemented in order to meet the  
 70 desired properties of the resonator. After these  
 71 modifications were completed, the resonant fre-  
 72 quency of the prototype was tuned to 24.25 MHz,  
 73 the quality factor achieved 70% of the expected  
 74 value and the field amplitude distribution along  
 75 the structure was uniform within  $\pm 2\%$ . Complete  
 76 specifications for the final design of the full-power  
 77 prototype have been established.

#### Acknowledgments

78  
 79  
 80  
 81 We would like to address our thanks to S.I.  
 82 Sharamentov (ATLAS-ANL), A. Barcikowski, E.  
 83 Rotela and B. Rusthoven (TD-ANL) and H.  
 84 Friedsam (ASD-ANL) for their valuable help.  
 85

#### References

- 86  
 87  
 88  
 89  
 90  
 91  
 92  
 93  
 94  
 95  
 96  
 97  
 98  
 99  
 100
- [1] V.V. Vladimírsky, Prib. Tekh. Eksp 3 (1956) 35.
  - [2] D.A. Swenson, Proceedings of the 1994 Linac Conference, Tsukuba, Japan, August 21–26, 1994, p. 804.
  - [3] U. Ratzinger. Proceedings of the 1988 Linac Conference, October 3–7, Newport News, Virginia, CEBAF Report 89-001, 1988, p. 185.
  - [4] P.N. Ostroumov, et al., Proceedings of the 2001 PAC Conference, June 18–22, Chicago, IL, USA, 2001, p. 4077.

- 1 [5] E.S. Masunov, N.E. Vinogradov, *Phys. Rev. Special*  
2 *Topics—Accelerators Beams* 7 (2001) 070101.
- 3 [6] U. Ratzinger, *Proceedings of the 1991 PAC Conference*,  
4 May 6–9, San-Francisco, CA, USA, 1991, p. 567.
- 5 [7] P.N. Ostroumov, et al., *Nucl. Instr. and Meth. B* 204  
6 (2003) 433.
- 7 [8] J.A. Nolen, *Nucl. Phys. A* 734 (2004) 661.
- 8 [9] K.W. Shepard, W.C. Sellyey, *Proceedings of the 1996*  
9 *Linac Conference*, August 26–30, Geneva, Switzerland,  
10 CERN 96-07, 1996, p. 68.
- 11 [10] M.P. Kelly, et al., *Proceedings of the 2001 PAC*  
12 *Conference*, June 18–22, Chicago, IL, USA, 2001, p. 506.
- 13 [11] A.A. Kolomiets, et al., *Proceedings of the XVI European*  
14 *Particle Accelerator Conference*, Stockholm, Sweden, June  
15 22–26, 1998, p. 1201.
- [12] Scientific Instrument Services, Inc., <http://www.simion.com/>
- [13] P.N. Ostroumov, V.N. Aseev, B. Mustapha, *Beam Loss*  
16 *Studies in High-Intensity Heavy-Ion Linacs*, *Phys. Rev.*  
17 *Special Topics—Accelerators Beams* 7, 090101.
- [14] CST EMS. <http://www.cst.de/>
- [15] M. Portillo, et al., *Proceedings of the 2001 PAC*  
18 *Conference*, June 18–22, Chicago, IL, USA, 2001, p. 3015.
- [16] A. Moretti, et al., *Proceedings of the 1981 Linac*  
19 *Conference*, October 19–23, Santa Fe, New Mexico, LA-  
20 9234-C, 1981, p. 197.
- [17] CST MWS. <http://www.cst.de/>
- [18] N.E. Vinogradov, et al., *Proceedings of the 2003 PAC*  
21 *Conference*, May 12–16, Portland, OR, USA, 2003, p.  
22 2790.
- [19] <http://www.balseal.com/index.jsp>.
- [20] <http://www.technit.de>.

UNCORRECTED PROOF